



Cite this: *Chem. Sci.*, 2025, **16**, 14635

All publication charges for this article have been paid for by the Royal Society of Chemistry

Received 3rd June 2025  
Accepted 9th July 2025

DOI: 10.1039/d5sc04037j  
[rsc.li/chemical-science](http://rsc.li/chemical-science)

## Synthesis of monodisperse inorganic polyphosphate polyP<sub>10</sub> via a photocaging strategy†

Sandra Moser,<sup>a</sup> Gloria Hans,<sup>a</sup> Jiahui Ma,<sup>a</sup> Thomas Haas,<sup>a</sup> Nikolaus Jork,<sup>a</sup> Felix Bauer,<sup>a</sup> Bernhard Breit <sup>a</sup> and Henning J. Jessen <sup>ab</sup>

Inorganic polyphosphate (polyP), a linear biopolymer composed only of orthophosphate units, has emerged as a molecule of critical biological importance across species. While commercially available polyPs are polydisperse mixtures – irrespective of their origin (chemical, biochemical) – recent strategies have focused on the bottom-up synthesis of monodisperse polyPs that have distinct advantages in mechanistic studies. However, until now, syntheses have been limited to defined chains of up to eight phosphate units due to challenges in deprotection-associated degradation and purification. Here, we disclose a new strategy based on two terminal coumarin photocages to synthesize the longest monodisperse polyP chain available to date: polyP<sub>10</sub>. The photoremovable protecting groups facilitate purification and enable efficient deprotection with light. By tuning the photocage, we achieve control over uncaging wavelengths, integrate targeting modifications and incorporate <sup>18</sup>O-labels. This is the first example of a photouncaging strategy in which an <sup>18</sup>O-labeled photocage is specifically designed to release an <sup>18</sup>O-labeled metabolite for downstream applications. During the uncaging, we observe an unprecedented aromatic substitution reaction from a cleaved coumarin photocage cation onto the second photocage that is still attached to the polyP chain. This suggests a  $\pi$ -stacking facilitated loop-like arrangement of caged polyP in water that is supported by DFT calculations.

## Introduction

Inorganic polyphosphate (polyP), a linear polymer composed of three up to thousands of orthophosphates, has evolved from its former status as a “forgotten polymer” 30 years ago<sup>1</sup> to a molecule of critical biological and technological importance. Today it is known that this conserved biopolymer is involved in fundamental cellular processes<sup>2</sup> such as energy metabolism,<sup>3</sup> stress response<sup>4</sup> and DNA damage repair.<sup>5</sup> Additionally, it holds biomedical relevance<sup>6</sup> as it plays a role in blood clotting,<sup>7</sup> inflammation,<sup>8</sup> bone regeneration<sup>9</sup> and bacterial virulence.<sup>10</sup> PolyP has been shown to covalently and non-covalently bind to certain protein domains.<sup>11</sup> Commercially available polyP is manufactured through two main methods: chemical synthesis and enzymatic synthesis.

In the chemical process, sodium monophosphate is heated to 700–1000 °C with subsequent rapid cooling.<sup>12</sup> This technique yields a glass-like mixture of polyphosphates with different chain lengths,<sup>13</sup> known as Graham’s salt or – misguiding because of its linear structure – as sodium hexametaphosphate.<sup>14</sup> By varying the temperature and vapor pressure, the average chain length can be

adjusted.<sup>12</sup> Moreover, different modifications have been obtained in the solid state, usually showing a helical arrangement of the polymer; based on these reports, such arrangements have also been suggested in solution.<sup>15</sup>

PolyP can also be synthesized enzymatically. Certain organisms, including yeast, bacteria and algae store high quantities of polyphosphates, which can be isolated through methods like phenol/chloroform extraction.<sup>12</sup> Recently, an optimized extraction protocol has also become available for mammalian cells.<sup>16</sup> While not yet commercially available, innovative biotechnological methods have demonstrated the potential to use *Saccharomyces cerevisiae* to convert phosphate-rich wastewater<sup>17</sup> or de-oiled seeds and bran<sup>18</sup> into sodium polyphosphate. These production methods have all in common, that they provide polyP samples with mixed chain lengths, making it hard to apply precise analytical techniques like mass spectrometry.

The isolation of polyPs with a defined chain-length is currently not possible with the methods described above, but recent advances have enabled the synthesis of short-chain polyPs up to eight phosphate units on mg to g scale (Scheme 1). Pure tetra- to octapolypophosphoric acid, resulting in a polyP mixture with an average chain length of around five (Scheme 1a).<sup>19</sup> Separation is achieved through multiple extraction steps combined with cation- and anion-exchange chromatography making this process highly labor-intensive.<sup>19</sup> The bottom-up synthesis of

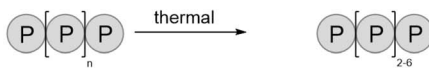
<sup>a</sup>Institute of Organic Chemistry, Albert-Ludwigs-Universität Freiburg, Albertstraße 21, 79104 Freiburg im Breisgau, Germany. E-mail: [henning.jessen@oc.uni-freiburg.de](mailto:henning.jessen@oc.uni-freiburg.de)

<sup>b</sup>CIBSS – Centre for Integrative Biological Signalling Studies, Albert-Ludwigs-Universität Freiburg, Schänzelstraße 18, 79104 Freiburg im Breisgau, Germany

† Electronic supplementary information (ESI) available. See DOI: <https://doi.org/10.1039/d5sc04037j>



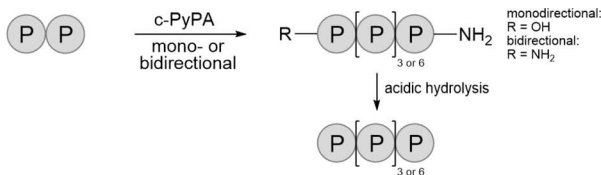
## a) from polyphosphoric acid (Griffith &amp; Buxton 1967)



## b) P-amidite homologative approach (Cremosnik &amp; Jessen 2014/2021)



## c) c-PyPA and acidic hydrolysis approach (Singh &amp; Jessen 2019)

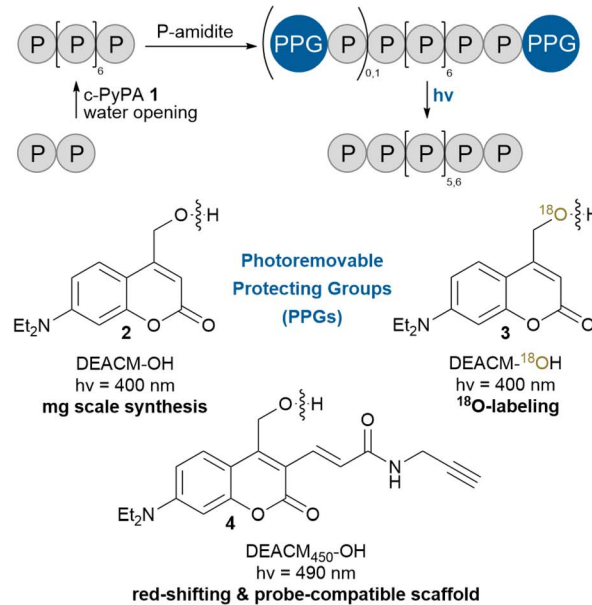


## challenges of a-c :

- laborious separation procedure
- base or acidic induced removal of protecting groups / hydrolysis
- so far limited to chain-lengths up to 8 phosphate units

d) this work: first polyP<sub>9</sub> & polyP<sub>10</sub> synthesis

combining b), c) &amp; photolysis



## advantages of d :

- facilitated purification of photocaged polyP<sub>9/10</sub>
- efficient PPG removal by light irradiation
- setting a record for the synthesis of the longest defined polyP

Scheme 1 Overview of chemical synthesis strategies for defined unmodified short-chain polyPs.

defined polyPs is possible using a P-amidite homologative approach (Scheme 1b).<sup>20</sup> This process builds on three steps: activation/coupling, oxidation and base-induced deprotection, which can be performed in a single flask, and can be repeated iteratively.<sup>20a,21</sup> To enhance efficiency, an improved approach was developed using the triphosphorylation reagent cyclic pyrophosphoryl P-amidite 1 (c-PyPA, Scheme 1c and 2).<sup>20b,22</sup>

This reagent enables the simultaneous incorporation of three phosphate units in a monodirectional approach or six in a bidirectional approach. The three-steps – activation/coupling, oxidation and linearization by nucleophiles – can be carried out in one pot as well. Amines are particularly effective for linearization. Starting from pyrophosphate, one then has direct access to symmetrical polyP<sub>8</sub>-diamidates, which can be hydrolyzed in acidic conditions to yield unmodified monodisperse polyP<sub>8</sub>.<sup>22a,23</sup> While additional polyphosphorylation reagents exist for the synthesis of terminally modified oligophosphates,<sup>24</sup> including nucleoside tetra- to heptaphosphates,<sup>25</sup> dinucleoside tetra- and penta-phosphates<sup>24c,25a,26</sup> as well as oligophosphorylated peptides,<sup>27</sup> none of them have yet been used to synthesize unmodified polyP. To date, no monodisperse polyPs with chain lengths longer than eight units have been successfully synthesized. Achieving this would be an important step towards covering additional biological polyP structures, thus enabling more precise analysis<sup>28</sup> and enhancing our understanding of their metabolic functions and topology. Defined longer chains will serve for precise analytical assignments and can help to understand and quantify polyP binding to proteins.

The synthetic limitation arises from the complexity of acquiring suitably long phosphate precursors and the increasing difficulty in purifying and isolating well-defined, elongated, non-UV active polyphosphates.<sup>29</sup>

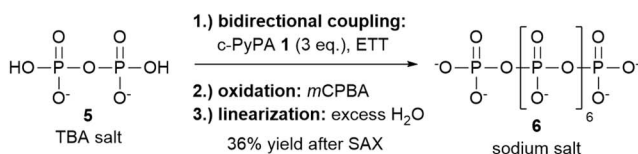
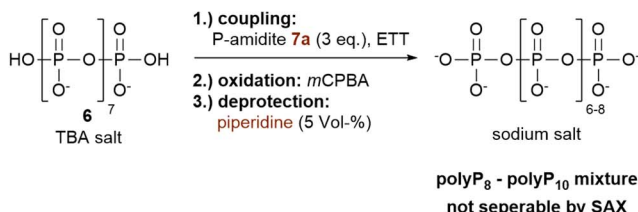
Herein, we address these challenges by developing a novel strategy, which extends one-step-synthesized polyP<sub>8</sub> to monodisperse and unmodified polyP<sub>9</sub> and polyP<sub>10</sub> *via* photocaged polyP<sub>9</sub> and polyP<sub>10</sub> (Scheme 1d). The photoremoveable protecting groups are crucial for their separation and enable efficient deprotection by light irradiation, avoiding decomposition observed with chemically triggered deprotection. Additionally, by tuning the photoremoveable protecting groups, our approach allows for adjustment of the uncaging wavelength, the addition of clickable residues for probe development and the incorporation of <sup>18</sup>O-labels to create heavy derivatives of polyP<sub>9</sub> and polyP<sub>10</sub> underlining the versatility of the approach. During the photo-uncaging experiments, we observed an unprecedented aromatic substitution on one photocage by the primary coumarin cation of another, indicating the formation of a loop-like structure in the polyP chain, likely stabilized by  $\pi$ -stacking interactions between the coumarin cages, aligning them in close proximity.

## Results and discussion

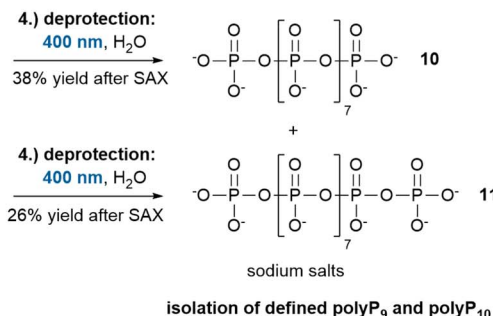
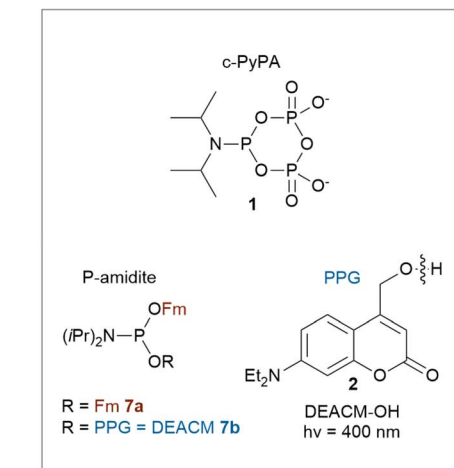
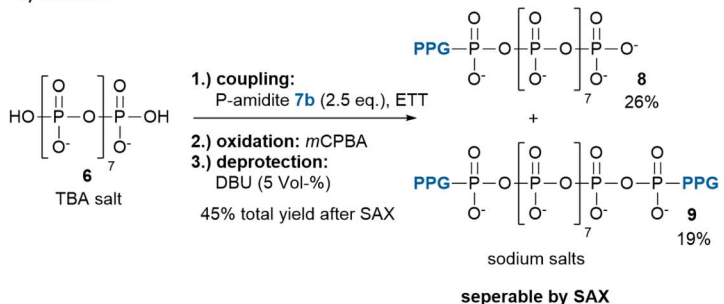
Chemical synthesis of polyP<sub>9</sub> and polyP<sub>10</sub>

PolyP<sub>8</sub> 6 was synthesized in a single step starting from pyrophosphate 5, using the bidirectional approach with c-PyPA 1 (Scheme 2a). Direct water-mediated ring opening to polyP<sub>8</sub> 6 has



a) direct access to polyP<sub>8</sub> as starting material for polyP<sub>9/10</sub> synthesisb) problems of polyP<sub>9/10</sub> synthesis

## c) solution



**Scheme 2** Syntheses of polyP<sub>8</sub>, polyP<sub>9</sub> and polyP<sub>10</sub>. (a) One-step synthesis of polyP<sub>8</sub> 6 via the bidirectional c-PyPA approach with water-induced ring opening. (b) Attempted synthesis of polyP<sub>9</sub> and polyP<sub>10</sub> using the bidirectional P-amidite method with a standard P-amidite 7a followed by piperidine deprotection,<sup>20b</sup> yielding a non-separable polyP<sub>8</sub>, polyP<sub>9</sub> and polyP<sub>10</sub> mixture using SAX. (c) Successful synthesis of polyP<sub>9</sub> 10 and polyP<sub>10</sub> 11 via photolysis of their photocaged derivatives 8 and 9, which are separable by SAX, employing a photocaged P-amidite 7b. Abbreviations: TBA: tetrabutylammonium, ETT: 5-(ethylthio)-1*H*-tetrazole, *m*CPBA: *meta*-chloroperbenzoic acid, Fm: fluorenylmethyl, PPG: photoremoveable protecting group, DBU: 1,8-diazabicyclo[5.4.0]undec-7-ene.

been low-yielding previously, while amine-induced linearization followed by acidic hydrolysis was more effective.<sup>22a</sup> The modified approach described herein provides direct access to unmodified polyP<sub>8</sub> by quenching the reaction mixture into excess of water, resulting in clean linearization to polyP<sub>8</sub> 6.

To extend this readily available polyP<sub>8</sub> (235 mg synthesized in a single step) to polyP<sub>10</sub>, the bidirectional P-amidite approach can be used.<sup>20b</sup> However, this strategy presents two main challenges: first, the basic conditions required to remove the fluorenylmethyl (Fm) protecting groups from the newly introduced terminal phosphates can lead to partial degradation of the polyP chain. Second, the resulting mixture of polyP<sub>8</sub>, polyP<sub>9</sub> and polyP<sub>10</sub> is difficult to separate effectively by strong anion exchange chromatography (SAX) and hard to assign analytically (Scheme 2b). To overcome these limitations, a P-amidite bearing only one Fm group and a photoremoveable protecting group (photocage) was employed enabling milder and orthogonal cleavage (Scheme 2c). The coumarin derivative DEACM-OH 2 was chosen due to its well-established photocleavage mechanism and its straightforward three-step synthesis.<sup>30</sup> Reaction of the P-amidite 7b (2.5 eq.) with polyP<sub>8</sub> 6 followed by oxidation

and careful Fm removal gave a mixture of mono-photocaged polyP<sub>9</sub> 8 (26% yield) and bis-photocaged polyP<sub>10</sub> 9 (19% yield) in a ratio of approx. 1.4 : 1. Increasing the amount of P-amidite 7b to 3 eq. shifted the product distribution strongly in favour of bis-photocaged polyP<sub>10</sub> 9 with a product ratio of 8 to 9 of approx. 0.1 : 1. The two products were readily separated by SAX. UV-activity of these compounds greatly facilitated purification. While their proton NMR chemical shifts are very similar, <sup>31</sup>P-NMR provided a clear distinction: unsymmetrical mono-caged polyP<sub>9</sub> 8 shows an integration ratio of 1 : 1 : 7, whereas 9 shows a 2 : 8 pattern. This confirms the symmetrical dual-caged structure of the latter (ESI,† for a <sup>31</sup>P-NMR chemical shift table for condensed phosphates see Accounts Chem. Res. 20b). Irradiation of 8 and 9 at  $\lambda = 400$  nm released defined polyP<sub>9</sub> 10 or polyP<sub>10</sub> 11, respectively, without requiring acid or base treatment. The reaction proceeded cleanly; however, precipitation followed by extensive washing failed to completely remove the DEACM-OH 2 cleavage product, resulting in the isolation of a yellow-brown precipitate. Therefore, purification via SAX was required, which led to significant losses and ultimately reduced the yields to 38% for 10 and 26% for 11, respectively.

Importantly, this new synthesis approach conceptually allows for further extension of the polyP chain by using polyP<sub>9</sub> or polyP<sub>10</sub> as starting materials.

### An unexpected quasi-intramolecular reaction during the uncaging process

It is possible to track the uncaging process (Fig. 1a) in water by <sup>31</sup>P-NMR. This requires high concentrations (approx. 10 mM) to detect the phosphate resonances of the termini. As expected, during polyP<sub>9</sub> release from mono-caged polyP<sub>9</sub> **8**, the ratio of the free phosphate signal to the caged phosphate signal gradually shifted from 1:1 to 2:0 over time (Fig. 1b and ESI-2a†). However, this process was slow, taking approximately 7 h to completion, as the cleaved DEACM-OH **2** chromophore competes for light absorption and is poorly water soluble, leading to precipitation and an opaque reaction mixture. A more practical approach was to conduct the reaction at lower concentration, such as 2 mM or less, and track its progress by capillary electrophoresis coupled to mass spectrometry<sup>31</sup> (CE-MS, Fig. 1c and ESI-2b†). Dilution significantly shortens the reaction time to 90 min.

A similar behaviour as discussed above was expected for the bis-photocaged polyP<sub>10</sub> **9** (Scheme 3a). The reaction should proceed through the mono-photocaged polyP<sub>10</sub> intermediate **12**. However, interestingly, a new main distinct peak appeared after a very short irradiation time in the CE-MS profile in addition to the peaks for the starting material **9**, mono-caged polyP<sub>10</sub> **12** and the free polyP<sub>10</sub> **11** both at 2 mM of **9** (Scheme

3b and Fig. ESI-3a†), as well as at 100  $\mu$ M of **9** (Fig. ESI-3b†). This new peak represents a constitutional isomer with the exact same mass as the starting material **9**. The new isomer could still be further cleaved under irradiation to yield polyP<sub>10</sub> **11** albeit at a reduced rate. The reaction (2 mM) was complete after approximately 5 h of irradiation. Literature reports that coumarins can undergo reversible [2 + 2] cycloadditions<sup>30c,32</sup> or decarboxylation<sup>30c,33</sup> under UV light, the latter ruled out by the requirement of identical mass. Thus, the [2 + 2] cycloaddition would be a viable explanation. However, the expected cycloadduct would no longer function as a photocage, which contradicts our observations. Yet, regeneration of the cage and cleavage might be a result of a [2 + 2] cycloreversion. To identify the intermediate, it was generated by stopping the reaction after 1 h irradiation time, when it had accumulated next to polyP<sub>10</sub> **11**, followed by isolation *via* SAX. Full NMR characterization suggested the formation of the substitution product **13** (Scheme 3). The proposed mechanism, illustrated in Scheme 3c, is also supported by DFT calculations (Fig. 2, [BP86/def2SVP-D3BJ-SMD(water)]). It starts with the photolysis of bis-DEACM-caged polyP<sub>10</sub> **9**. Coumarin photocages are believed to operate through the heterolysis of the DEACM-OP bond in the excited state. This generates a contact ion pair<sup>34</sup> consisting of the primary DEACM cation **15** and its conjugated base, the anion of the leaving group **16**.<sup>35</sup> Unlike typical pathways where the cation would either quickly recombine with the anion or be intercepted by the solvent water after escape from the contact ion pair,<sup>35</sup> **15** and **16** instead undergo an electrophilic aromatic substitution (ArSE). The reaction proceeds through Wheland

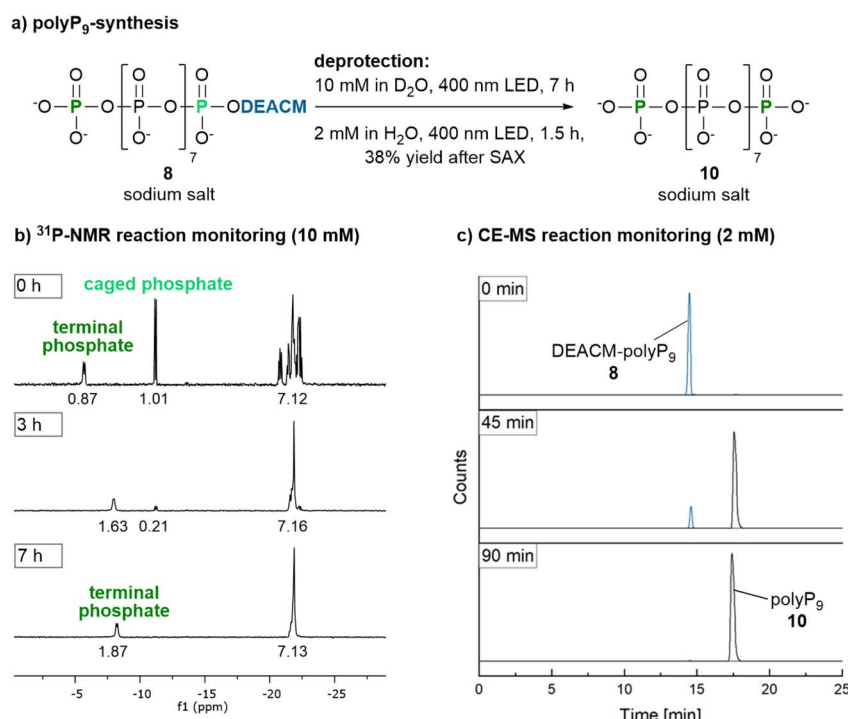
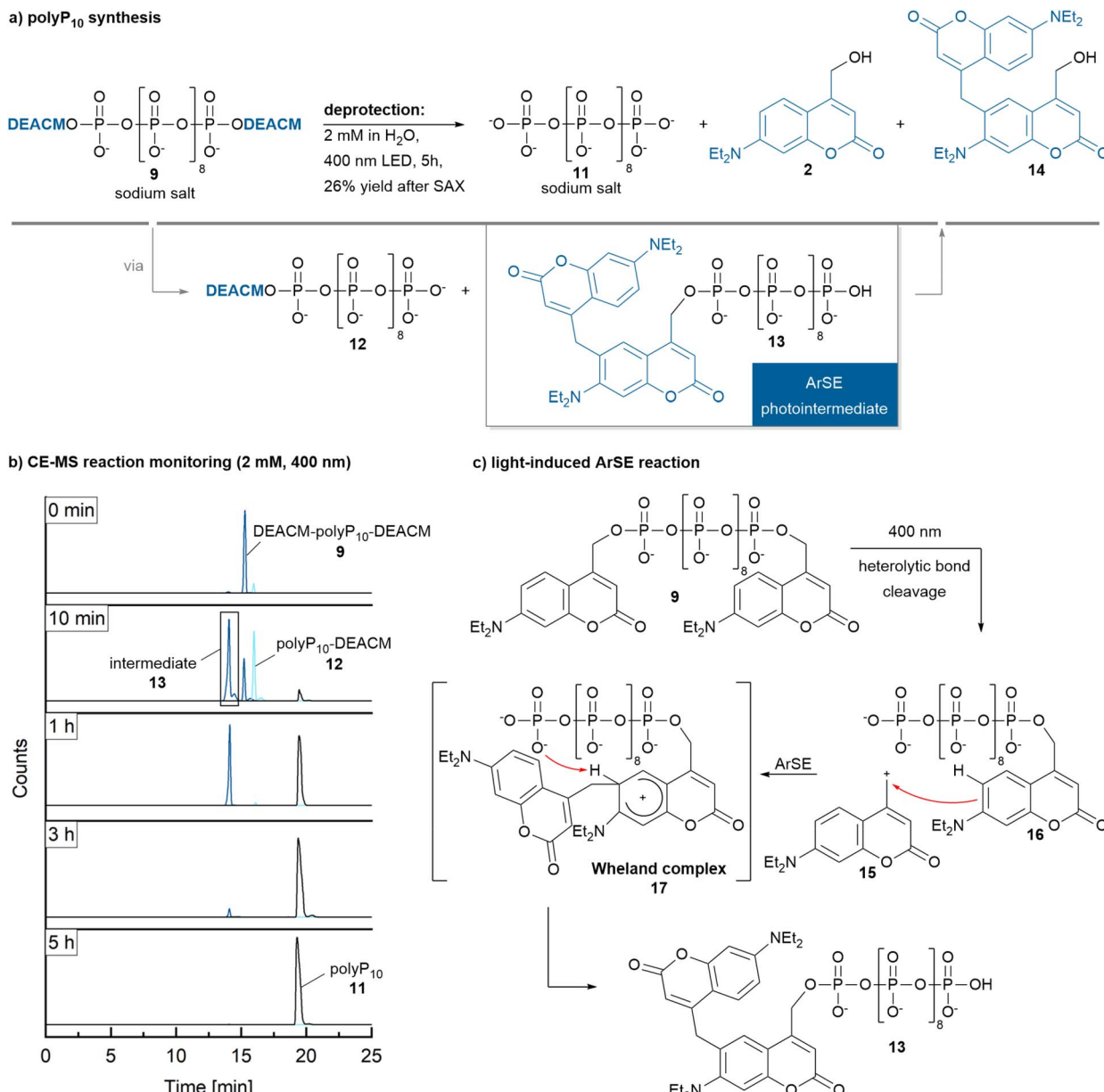


Fig. 1 (a) Photorelease of polyP<sub>9</sub> **10** from **8** at 400 nm. (b) At 10 mM in H<sub>2</sub>O, <sup>31</sup>P-NMR monitoring indicated complete photorelease after approx. 7 h. (c) At a lower concentration of 2 mM in H<sub>2</sub>O, CE-MS monitoring (with sample dilution to 500  $\mu$ M prior to analysis), showed completion of cleavage after approx. 90 min. Detailed time courses are available in Fig. ESI-2-†.





**Scheme 3** (a) Photorelease of polyP<sub>10</sub> **11** from **9** (2 mM in H<sub>2</sub>O) at 400 nm. (b) CE-MS reaction monitoring (sample dilution to 500  $\mu$ M prior to analysis) revealed complete photorelease within 5 h, proceeding through two intermediates, **12** and **13**. (c) The formation of **13** is proposed to be a quasi-intramolecular ArSE reaction, occurring after the cleavage of one of the two photoremoveable protecting groups from a loop-like pre-oriented structure (see Fig. 2). Evidence for the release of the byproducts **2** and **14** is provided in Fig. ESI-4.†

complex **17**, in which a phosphate group oxygen abstracts the aromatic proton (Fig. 2). For this quasi-intramolecular reaction to occur, the two DEACM residues must be in close proximity, as otherwise the primary cation generated during photoheterolysis rapidly reacts with water.<sup>34</sup> This suggests that in the starting material **9**, the polyP<sub>10</sub> chain adopts a loop-like conformation, stabilized by  $\pi$ -stacking interactions between the DEACM-modifications in the polar solvent water. Since the newly formed intermediate **13** retains the coumarin photocage structure, prolonged irradiation leads to the release of unmodified polyP<sub>10</sub> **11**, albeit more slowly, potentially as a result of more

efficient relaxation pathways. Indeed, HRMS analysis of the fully deprotected polyP<sub>10</sub> reaction mixture – lyophilized after light irradiation and redissolved in DCM – revealed the presence of the final cleavage product **14** alongside DEACM-OH **2** (Fig. ESI-4†). Examples in which the contact ion pair of a coumarin-caged compound undergoes reaction pathways beyond simple recombination to the starting material or solvent trapping have been reported. These include an intramolecular cyclization rearrangement in styryl-substituted coumarins<sup>36</sup> and deprotonation of a tertiary coumarin cation yielding an alkene rather than the expected alcohol.<sup>34</sup> Photocleavage of

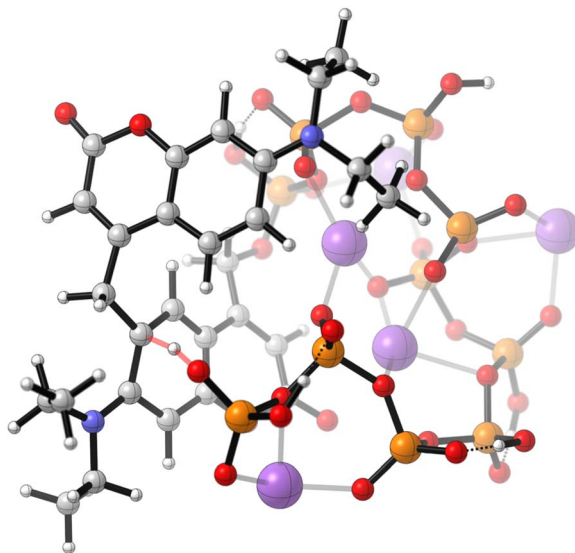
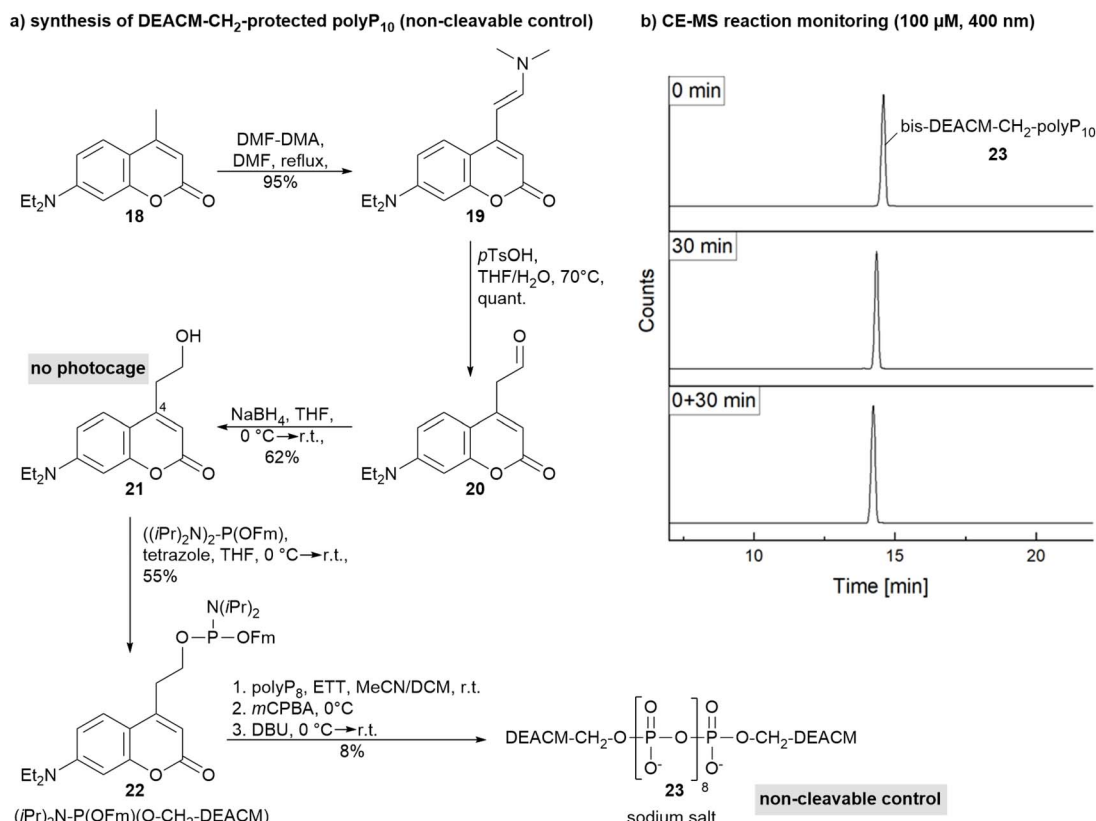


Fig. 2 Calculated transition state of the proton abstraction (red bonds) in Wheland complex 17 supporting a loop-like structure of the polyP<sub>10</sub> chain (P: orange, O: red). The counterions are Na<sup>+</sup> (purple). [BP86/def2SVP-D3BJ-SMD(water)].

a trimethylsilyl-substituted coumarin-based photocage also affords an alkene by either intramolecular silylcarbonylation, hydrolysis or Peterson-type desilylation after photoexcitation.<sup>37</sup> Photo-Claisen rearrangements that impair release efficiency have also been observed in coumarin-caged tyrosine<sup>38</sup> and 4-hydroxytamoxifen analogues.<sup>39</sup> ArSE reactions have not been previously described.

To further demonstrate that the light-induced heterolysis of the DEACM-OP bond is essential for side-product formation in our system, bis-DEACM-CH<sub>2</sub>-protected polyP<sub>10</sub> 23 was synthesized (Scheme 4a) and irradiated at  $\lambda = 400$  nm (Scheme 4b and Fig. ESI-5†). In this derivative, the DEACM carbon chain at position 4 is extended by one CH<sub>2</sub> group, eliminating its uncaging pathways, while still potentially enabling the known [2 + 2] cycloaddition of coumarins. Electropherograms showed no additional peak with the same mass (Scheme 4b and Fig. ESI-5†), confirming that ArSE product formation did not occur under these conditions and requires primary cation generation in a contact ion pair. Extended irradiation (beyond 2 h) led to decomposition, resulting in a mixture of undefined products. The synthesis of DEACM-CH<sub>2</sub>-OH 21 was accomplished in three steps, starting from commercially available coumarin 18 via enamine formation, hydrolysis and reduction (Scheme 4a).



**Scheme 4** (a) Synthesis of bis-DEACM-CH<sub>2</sub>-protected polyP<sub>10</sub> 23 as non-cleavable control. (b) CE-MS reaction monitoring shows no formation of an isobaric product. Abbreviations: DMF-DMA: *N,N*-dimethylformamide dimethyl acetal, DMF: dimethylformamide, *p*TsOH: *p*-toluenesulfonic acid, THF: tetrahydrofuran, Fm: fluorenylmethyl, ETT: 5-(ethylthio)-1*H*-tetrazole, DCM: dichloromethane, *m*CPBA: *meta*-chloroperbenzoic acid, DBU: 1,8-diazabicyclo[5.4.0]undec-7-ene.



Table 1 Photophysical properties in H<sub>2</sub>O

polyP	Absorption $\lambda_{\max}^a$ /nm	$\varepsilon_{\max}^b$ /(M <sup>-1</sup> cm <sup>-1</sup> )	Emission $\lambda_{\max}^c$ /nm
DEACM-polyP <sub>9</sub> <b>8</b>	386	16 340	445, 491, 527
<sup>18</sup> O-DEACM-polyP <sub>9</sub> <b>34</b>	386	16 220	445, 491, 527
Bis-DEACM-polyP <sub>10</sub> <b>9</b>	382	20 280	440, 490, 527
Bis- <sup>18</sup> O-DEACM-polyP <sub>10</sub> <b>35</b>	382	26 440	440, 490, 527
Bis-DEACM-CH <sub>2</sub> -polyP <sub>10</sub> <b>23</b>	381	21 060	437, 474
Bis-DEAC <sub>450</sub> -polyP <sub>10</sub> <b>24</b>	438	28 474	523, 543
Bis-TPP-DEAC <sub>450</sub> -polyP <sub>10</sub> <b>27</b>	441	16 975	520, 542

<sup>a</sup> Wavelength of the absorption maximum, 50  $\mu$ M. <sup>b</sup> Molar extinction coefficient at the absorption maximum  $\lambda_{\max}$ . <sup>c</sup> Wavelength of the emission maxima upon excitation at the absorption maximum, 100 nM.

The protected polyP<sub>10</sub> **23** exhibits an absorption maximum at 381 nm and two fluorescence maxima of 437 nm and 474 nm. The presence of multiple emission maxima, not only in **23**, but also in the mono-DEACM-caged polyP<sub>9</sub> **8** and bis-DEACM-caged polyP<sub>10</sub> **9** (Table 1), may be explained by the existence of chromophore  $\pi$ -stacking interactions. This supports not only a loop-like arrangement of the polyP chain in bis-caged molecules, but highlights the potential for intermolecular interactions leading to supramolecular aggregation.<sup>40</sup> Bis-DEACM-CH<sub>2</sub> protected polyP<sub>10</sub> **23** is the first example of a fluorophore end-labeled monodisperse double-digit polyP and may have versatile applications, such as fluorescence-based tracking of cellular uptake and direct fluorescent detection of polyphosphorylated proteins on gels without the need for staining methods.

### Synthesis of clickable, red-shifted photocaged polyP<sub>10</sub>

Bis-DEACM-photocaged polyP<sub>10</sub> **9** has an absorption maximum at 382 nm (Table 1) and can be cleaved with a 400 nm LED. However, for specific applications, such as cellular studies, red-shifted activation is preferred to high-energy UV light. Visible light has better tissue penetration and has reduced photo-toxicity to cells.<sup>41</sup> By using different photocages, our synthetic approach allows for easy tuning of these parameters. Moreover, targeting moieties and modifications that enhance cellular uptake could be installed.<sup>42</sup> Intracellular delivery of polyP into cells has previously been achieved using polycationic molecular transporters by non-covalent polyplex formation.<sup>43</sup> Choosing clickable<sup>42</sup> DEAC<sub>450</sub>-OH<sup>44</sup> **4** instead of DEACM-OH **2** as photocage on the P-amidite, a photocaged polyP<sub>10</sub> **24** with an absorption maximum around 438 nm was obtained (Fig. 3a and Table 1). Additionally, it features a clickable handle for further probe development, such as organelle-specific targeting.<sup>45</sup> Interestingly, during the uncaging process with 490 nm light, the direct photorelease again competed with an ArSE reaction as identified by CE-MS, LC-MS and NMR (Fig. 3b and ESI-7†).

It likely follows the mechanism and required loop pre-arrangement proposed in Scheme 3c. While the bis-DEACM-polyP<sub>10</sub> ArSE intermediate **13** fully released free polyP<sub>10</sub> **11** (see Fig. ESI-3b†) within 60 min at a concentration of 100  $\mu$ M, the formation of the ArSE intermediate of bis-DEAC<sub>450</sub>-polyP<sub>10</sub> **25** significantly slowed down the polyP<sub>10</sub> **11** release, preventing

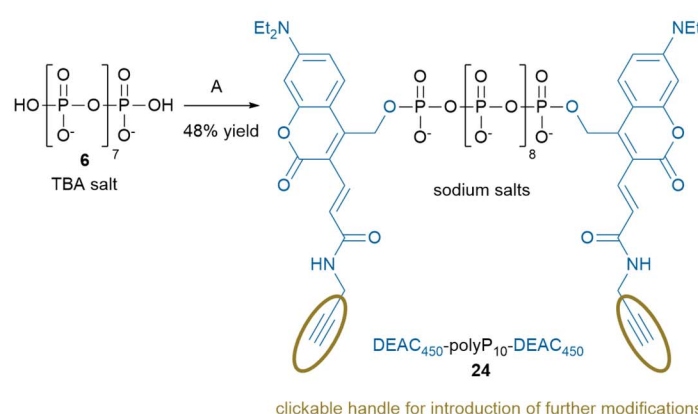
complete polyP<sub>10</sub> liberation even after 8 h irradiation at 100  $\mu$ M (Fig. 3b and ESI-6†). This may in part be attributed to the lower output power of the 490 nm LED (140 (mW)<sup>3</sup>) compared to the 400 nm LED (265 (mW)<sup>3</sup>), yet we surmise that additional rotational degrees of freedom for excited state inactivation and potentially energy transfer between the two chromophores followed by dissipation are also playing a role here. Notwithstanding, the reaction proceeded cleanly (see Fig. 3b), but at a much slower rate.

As an example for an organelle-targeting modification, we clicked<sup>46</sup> the mitochondria-targeting group triphenylphosphonium (TPP<sup>+</sup>) to the bis-DEAC<sub>450</sub>-polyP<sub>10</sub> **24** to obtain **27** (Fig. 3c). PolyP has been proposed to be produced by the mitochondrial F<sub>0</sub>F<sub>1</sub>-ATP synthase in mammalian cells,<sup>47</sup> and consequently its subcellular targeting for biological studies would be beneficial. However, the slow-release kinetics described above would be a major obstacle for further tool development. Even so, steric hindrance in the TPP<sup>+</sup> modified caged polyP in combination with coulombic repulsion of positive charges might reduce or obliterate the ArSE side reaction. Indeed, a 100  $\mu$ M solution of **27** exposed to 490 nm light fully released unmodified polyP<sub>10</sub> **11** within only 20 min (Fig. 3d and ESI-8†). The isobaric intermediate **28**, formed from **27**, did not significantly affect the photorelease kinetics and was not further characterized. These results indicate that **27** is, in principle, suitable for uncaging in living cells.

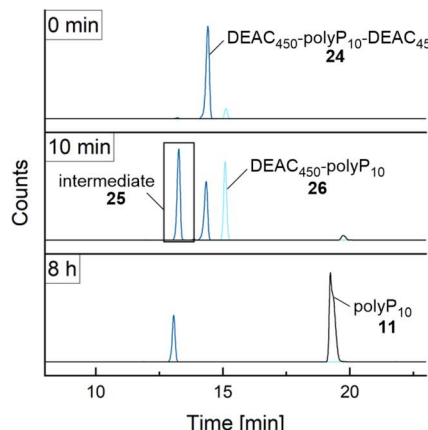
### Synthesis of <sup>18</sup>O-labeled polyP<sub>9</sub> and polyP<sub>10</sub>

We have recently demonstrated the use of <sup>18</sup>O-labeled phosphorylated metabolites as internal standards for quantitative CE-MS analysis.<sup>48</sup> Among available isotope labeling strategies, <sup>18</sup>O-labeling represents the only suitable approach for polyP, as oxygen is the only element with stable isotopes present in polyP. While Haas *et al.* achieved <sup>18</sup>O-labeling of polyP<sub>4</sub> using a base-labile P-amidite,<sup>48</sup> our synthesis method now enables the straightforward incorporation of <sup>18</sup>O-labels into the terminal phosphates of polyP<sub>9/10</sub> (and by extension beyond) by using <sup>18</sup>O-labeled DEACM-OH **3** as protecting group (Scheme 5). This heavy photocage was synthesized *via* Mitsunobo esterification of DEACM-OH **2** with <sup>18</sup>O-labeled 4-nitrobenzoic acid **31**, followed by hydrolysis based on a <sup>18</sup>O-labeling strategy for alcohols from Beddoe *et al.*<sup>49</sup> The corresponding

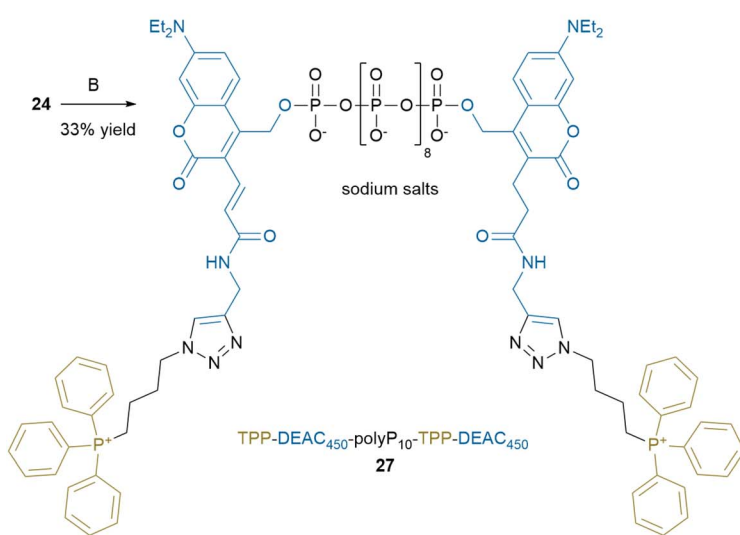


a) synthesis of red-shifted photocaged polyP<sub>10</sub>

## b) uncaging of 24



## c) further modification

e.g. introduction of mitochondria targeting group TPP<sup>+</sup>

## d) uncaging of 27

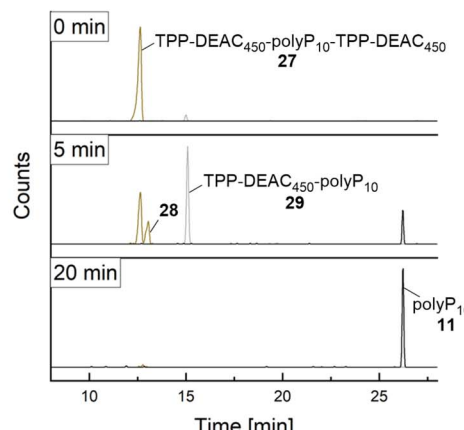
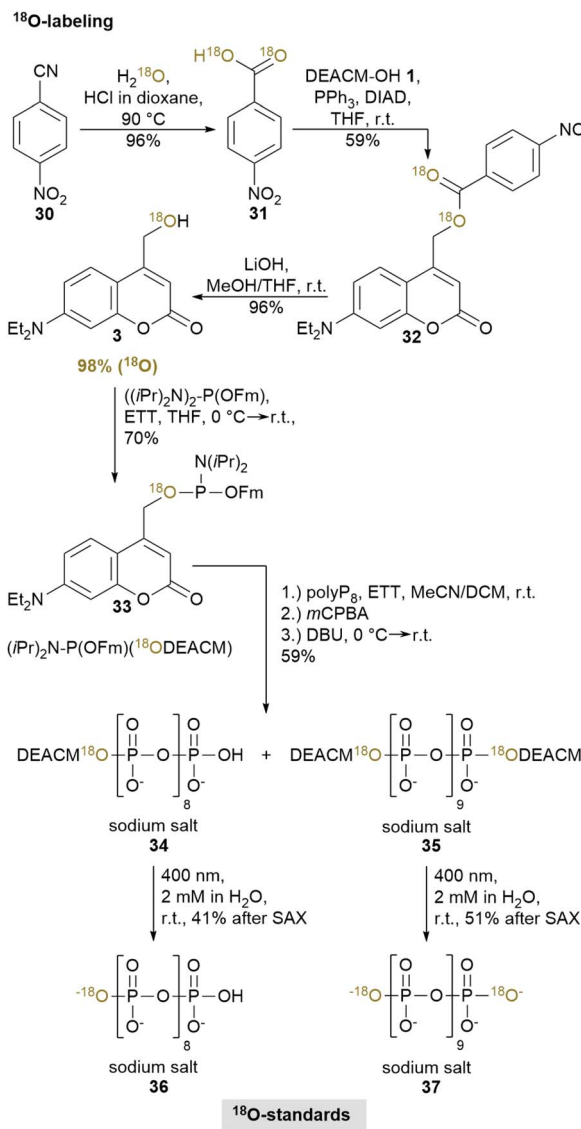


**Fig. 3** Synthesis and uncaging of red-shifted and modified caged polyP<sub>10</sub>'s. (a) Synthesis of bis-DEAC<sub>450</sub> caged polyP<sub>10</sub> 24. A: 1. (iPr)<sub>2</sub>N-P(OEt)<sub>2</sub>-DEAC<sub>450</sub> (3.0 eq.), ETT (20 eq.), MeCN/DCM, r.t., 30 min. 2. *m*CPBA (3.0 eq.), 0 °C, 20 min. 3. DBU (5 vol%), 0 °C → r.t., 1 h. (b) Photorelease of polyP<sub>10</sub> 11 from 24 (100 μM in H<sub>2</sub>O) at 490 nm. CE-MS reaction monitoring demonstrated that the photorelease proceeds through two intermediates, 25 and 26. The formation of 25 follows the mechanism suggested in Scheme 3. The photorelease process was slowed down through 25 and incomplete even after 8 h of irradiation. (c) Synthesis of bis-TPP-DEAC<sub>450</sub> caged polyP<sub>10</sub> 27. B: (4-azidobutyl)triphenyl phosphonium bromide (2.0 eq.), CuSO<sub>4</sub>·5H<sub>2</sub>O (1.0 eq.), THPTA (5.0 eq.), sodium ascorbate (10 eq.), 100 mM TEAA/DMSO, r.t., 3 h. (d) Photorelease of polyP<sub>10</sub> 11 from 27 (100 μM in H<sub>2</sub>O) at 490 nm. CE-MS reaction monitoring revealed complete photorelease within 20 min via mono-caged polyP<sub>10</sub> 29. The isobaric intermediate 28, formed from 27, was not isolated and identified. Abbreviations: Fm: fluorenylmethyl, ETT: 5-(ethylthio)-1*H*-tetrazole, DCM: dichloromethane, DMSO: dimethyl sulfoxide, *m*CPBA: *meta*-chloroperbenzoic acid, DBU: 1,8-diazabicyclo[5.4.0]undec-7-ene, TPP: triphenyl-phosphonium, THPTA: tris[(1-hydroxy-propyl-1*H*-1,2,3-triazol-4-yl)methyl]amine, TEAA: triethylammonium acetate.

photocaged P-amidite 33 was synthesized according to standard procedures.<sup>50</sup> Coupling 2.5 eq. of P-amidite 33 to polyP<sub>8</sub> 6 yielded a mixture of mono-<sup>18</sup>O-DEACM-polyP<sub>9</sub> 34 (20% yield) and bis-<sup>18</sup>O-DEACM-polyP<sub>10</sub> 35 (39% yield) which were well separable by SAX. Deprotection of 34 and 35 with 400 nm at 2 mM for 2 or 8 h, respectively, yielded <sup>18</sup>O-labeled polyP<sub>9</sub> 36 with 97% <sup>18</sup>O-isotope enrichment (5.8% natural abundance) or <sup>18</sup>O-labeled polyP<sub>10</sub> 37 with 95:5 (<sup>18</sup>O<sub>2</sub>:<sup>18</sup>O) isotope ratio (6.4% natural abundance). Importantly, these are the first

examples of an <sup>18</sup>O-labeled photocage designed specifically to release <sup>18</sup>O-labeled metabolites for downstream use, unlike previous strategies, where the label is incorporated during uncaging *via* <sup>18</sup>O-enriched water,<sup>35,51</sup> pre-installed in the biomolecule<sup>32</sup> or where the focus lies solely on the uncaging mechanism itself.<sup>53</sup> This <sup>18</sup>O-labeling approach can be adapted for the synthesis of diverse <sup>18</sup>O-labeled phosphorylated metabolites for use in biology, medicine and environmental science.





**Scheme 5** Synthesis of  $^{18}\text{O}$ -labeled polyP<sub>9</sub> 36 and  $^{18}\text{O}$ -labeled polyP<sub>10</sub> 37. Abbreviations: DIAD: diisopropyl azodicarboxylate, THF: tetrahydrofuran, Fm: fluorenylmethyl, ETT: 5-(ethylthio)-1*H*-tetrazole, DCM: dichloromethane, *m*CPBA: *meta*-chloroperbenzoic acid, DBU: 1,8-diazabicyclo[5.4.0]undec-7-ene.

## Conclusions

This study discloses the synthesis of two monodisperse poly-phosphates, polyP<sub>9</sub> and polyP<sub>10</sub>. It follows a new strategy to access for the first time polyP in the two-digit range. By generating photocaged versions, an effective separation of the different chain lengths in solution becomes possible. The uncaging process selectively releases the pure polyPs with defined chain length. It can be tracked conveniently with CE-MS in an aqueous environment.

During our study, we identified a novel photolysis side reaction involving quasi-intramolecular electrophilic aromatic substitution in bis-DEACM and bis-DEAC<sub>450</sub> caged polyP<sub>10</sub>, slowing down photorelease. This discovery suggests a loop-like

structure of the caged polyP<sub>10</sub> starting materials, possibly stabilized through  $\pi$ -stacking in water. The unique deactivation mechanism *via* ArSE for coumarin type photocages from the contact ion pair state<sup>34</sup> has not been described previously and is supported by DFT calculations. Importantly, the side-reaction can be reduced by introducing larger substituents on the photocage, such as TPP<sup>+</sup>.

Additionally, varying the photocage enables tailoring the uncaging wavelength and incorporating handles for further functional modifications. Both are paving the way for organelle-specific delivery of polyP<sub>10</sub> that can be released by light irradiation within cells, a focus for our future studies. Furthermore, utilizing an <sup>18</sup>O-labeled photocage allows for the introduction of <sup>18</sup>O into polyP<sub>9</sub> and polyP<sub>10</sub>, which can be applied as internal references in mass spectrometry. This strategy is readily extendable to the synthesis of other <sup>18</sup>O-labeled phosphorylated metabolites to allow their identification and quantification in complex biological samples *via* quantitative CE-MS. Their light-controlled release in living cells offers a tool to study intracellular dynamic phosphate turnovers and perturb cellular polyP metabolism.<sup>54</sup>

## Data availability

The data supporting this article have been included as part of the ESI.†

## Author contributions

S. Moser and H. Jessen designed the molecules. S. Moser and G. Hans synthesized most of the compounds. In addition, J. Ma, T. Haas, and N. Jork provided precursors. S. Moser characterized the compounds. F. Bauer performed DFT calculations. S. Moser drafted the initial manuscript and prepared the schemes and figures. B. Breit and H. Jessen reviewed the manuscript draft. H. Jessen conceived the project and provided feedback.

## Conflicts of interest

There are no conflicts to declare.

## Acknowledgements

We thank G. Liu, M. Lu and I. Prucker, A. Shukla from the Jessen group for help with CE and HRMS measurements. We also would like to thank Dr S. Braukmüller, Dr M. Keller and C. Warth from the Analytical Service Team of the University of Freiburg for NMR and HRMS measurements, respectively. This project was funded by the Deutsche Forschungsgemeinschaft (DFG, German Research Foundation, project number 445698446) in collaboration with the Indian Department of Biotechnology (DBT). Moreover, this work was supported by the Deutsche Forschungsgemeinschaft (DFG) under Germany's Excellence Strategy (CIBSS-EXC-2189-Project ID 390939984, to HJ).

## Notes and references

1 A. Kornberg, *J. Bacteriol.*, 1995, **177**, 491–496.

2 L. Xie and U. Jakob, *J. Biol. Chem.*, 2019, **294**, 2180–2190.

3 W. E. G. Müller, S. Wang, M. Neufurth, M. Kokkinopoulou, Q. Feng, H. C. Schröder and X. Wang, *J. Cell Sci.*, 2017, **130**, 2747–2756.

4 M. J. Gray and U. Jakob, *Curr. Opin. Microbiol.*, 2015, **24**, 1–6.

5 S. Bru, B. Samper-Martín, E. Quandt, S. Hernández-Ortega, J. M. Martínez-Láinez, E. Garí, M. Rafel, J. Torres-Torronteras, R. Martí, M. P. C. Ribeiro, J. Jiménez and J. Clotet, *DNA Repair*, 2017, **57**, 171–178.

6 X. Wang, H. C. Schröder and W. E. G. Müller, *J. Mater. Chem. B*, 2018, **6**, 2385–2412.

7 (a) S. A. Smith, N. J. Mutch, D. Baskar, P. Rohloff, R. Docampo and J. H. Morrissey, *Proc. Natl. Acad. Sci. U. S. A.*, 2006, **103**, 903–908; (b) D. Kudela, S. A. Smith, A. May-Masnou, G. B. Braun, A. Pallaoro, C. K. Nguyen, T. T. Chuong, S. Nownes, R. Allen, N. R. Parker, H. H. Rashidi, J. H. Morrissey and G. D. Stucky, *Angew. Chem., Int. Ed.*, 2015, **54**, 4018–4022.

8 S. A. Smith, S. H. Choi, J. N. R. Collins, R. J. Travers, B. C. Cooley and J. H. Morrissey, *Blood*, 2012, **120**, 5103–5110.

9 S. Omelon, J. Georgiou, Z. J. Henneman, L. M. Wise, B. Sukhu, T. Hunt, C. Wynnyckyj, D. Holmyard, R. Bielecki and M. D. Grynpas, *PLoS One*, 2009, **4**, e5634.

10 M. H. Rashid, K. Rumbaugh, L. Passador, D. G. Davies, A. N. Hamood, B. H. Iglewski and A. Kornberg, *Proc. Natl. Acad. Sci. U. S. A.*, 2000, **97**, 9636–9641.

11 (a) C. Azevedo, J. Singh, N. Steck, A. Hofer, F. A. Ruiz, T. Singh, H. J. Jessen and A. Saiardi, *ACS Chem. Biol.*, 2018, **13**, 1958–1963; (b) C. Azevedo, F. Borghi, X. B. Su and A. Saiardi, *Mol. Cell*, 2024, **84**, 1811–1815; (c) N. Neville, K. Lehotsky, K. A. Klupt, M. Downey and Z. Jia, *Mol. Cell*, 2024, **84**, 1802–1810; (d) A. Celik, F. Schöpf, C. E. Stieger, J. A. M. Morgan, S. Lampe, M. Ruwolt, F. Liu, C. P. R. Hackenberger, D. Roderer and D. Fiedler, *bioRxiv*, 2024, DOI: [10.1101/2024.07.29.605581](https://doi.org/10.1101/2024.07.29.605581).

12 B. Lorenzi and H. C. Schröder, in *Inorganic Polyphosphates Biochemistry, Biology, Biotechnology*, ed. H. C. Schröder and W. E. G. Müller, Mainz, Germany, 1st edn, 1999.

13 C. F. Callis, J. R. Van Wazer and P. G. Arvan, *Chem. Rev.*, 1954, **54**, 777–796.

14 (a) T. Graham, *Philos. Trans. R. Soc. London*, 1833, **123**, 253–284; (b) J. F. McCullough, J. R. V. Wazer and E. J. Griffith, *J. Am. Chem. Soc.*, 1956, **78**, 4528–4533.

15 (a) L. E. Jackson, B. M. Kariuki, M. E. Smith, J. E. Barralet and A. J. Wright, *Chem. Mater.*, 2005, **17**, 4642–4646; (b) K. Förg and H. A. Höppe, *Dalton Trans.*, 2015, **44**, 19163–19174; (c) R. Schoeppe, M. Waldmann, H. J. Jessen and T. Renné, *Biomolecules*, 2024, **14**, 937; (d) T. Glonek, *Origins Life Evol. Biospheres*, 2021, **51**, 1–60.

16 B. Lázaro, A. Sarrias, F. J. Tadeo, J. Marc Martínez-Láinez, A. Fernández, E. Quandt, B. Depares, T. Dürr-Mayer, H. Jessen, J. Jiménez, J. Clotet and S. Bru, *Methods*, 2025, **234**, 211–222.

17 J. Fees, J. J. Christ, S. Willbold and L. M. Blank, *Biotechnol. Bioeng.*, 2023, **120**, 456–464.

18 K. R. Herrmann, J. Fees, J. J. Christ, I. Hofmann, C. Block, D. Herzberg, S. Bröring, B. Reckels, C. Visscher, L. M. Blank, U. Schwaneberg and A. J. Ruff, *EFB Bioeconomy J.*, 2023, **3**, 100048.

19 E. J. Griffith and R. L. Buxton, *J. Chem. Soc.*, 1967, **89**, 2884–2890.

20 (a) G. S. Cremosnik, A. Hofer and H. J. Jessen, *Angew. Chem., Int. Ed.*, 2014, **53**, 286–289; (b) H. J. Jessen, T. Dürr-Mayer, T. M. Haas, A. Ripp and C. C. Cummins, *Acc. Chem. Res.*, 2021, **54**, 4036–4050.

21 H. J. Jessen, N. Ahmed and A. Hofer, *Org. Biomol. Chem.*, 2014, **12**, 3526–3530.

22 (a) J. Singh, N. Steck, D. De, A. Hofer, A. Ripp, I. Captain, M. Keller, P. A. Wender, R. Bhandari and H. J. Jessen, *Angew. Chem., Int. Ed.*, 2019, **58**, 3928–3933; (b) J. Singh, A. Ripp, T. M. Haas, D. Qiu, M. Keller, P. A. Wender, J. S. Siegel, K. K. Baldridge and H. J. Jessen, *J. Am. Chem. Soc.*, 2019, **141**, 15013–15017.

23 S. M. Hacker, M. Mex and A. Marx, *J. Org. Chem.*, 2012, **77**, 10450–10454.

24 (a) J. Y. Liao, S. Bala, A. K. Ngor, E. J. Yik and J. C. Chaput, *J. Am. Chem. Soc.*, 2019, **141**, 13286–13289; (b) S. M. Shepard and C. C. Cummins, *J. Am. Chem. Soc.*, 2019, **141**, 1852–1856; (c) S. M. Shepard, H. Kim, Q. X. Bang, N. Alhokbany and C. C. Cummins, *J. Am. Chem. Soc.*, 2021, **143**, 463–470.

25 (a) S. Mohamady and S. D. Taylor, *Org. Lett.*, 2013, **15**, 2612–2615; (b) G. Park, E. C. Wralstad, N. Faginas-Lago, K. Qian, R. T. Raines, G. Bistoni and C. C. Cummins, *ACS Cent. Sci.*, 2024, **10**, 1415–1422.

26 (a) Y. Ahmadibeni and K. Parang, *Org. Lett.*, 2007, **9**, 4483–4486; (b) Q. Han, B. L. Gaffney and R. A. Jones, *Org. Lett.*, 2006, **8**, 2075–2077.

27 K. Qian, B. Hanf, C. Cummins and D. Fiedler, *Angew. Chem., Int. Ed.*, 2025, e202419147.

28 S. K. Roy, S. Moser, T. Dürr-Mayer, R. Hinkelmann and H. J. Jessen, *Org. Biomol. Chem.*, 2025, **23**, 1373–1379.

29 S. M. Shepard, H. J. Jessen and C. C. Cummins, *J. Am. Chem. Soc.*, 2022, **144**, 7517–7530.

30 (a) V. Hagen, J. Bendig, S. Frings, T. Eckardt, S. Helm, D. Reuter and U. B. Kaupp, *Angew. Chem., Int. Ed.*, 2001, **40**, 1045–1048; (b) T. Weinrich, M. Gränz, C. Grünewald, T. F. Prisner and M. W. Göbel, *Eur. J. Org. Chem.*, 2017, **2017**, 491–496; (c) L. J. G. W. Van Wilderen, C. Neumann, A. Rodrigues-Correia, D. Kern-Michler, N. Mielke, M. Reinfelds, A. Heckel and J. Bredenbeck, *Phys. Chem. Chem. Phys.*, 2017, **19**, 6487–6496; (d) C. Hamerla, C. Neumann, K. Falahati, J. Von Cosel, L. J. G. W. Van Wilderen, M. S. Niraghatham, D. Kern-Michler, N. Mielke, M. Reinfelds, A. Rodrigues-Correia, A. Heckel, J. Bredenbeck and I. Burghardt, *Phys. Chem. Chem. Phys.*, 2020, **22**, 13418–13430.

31 D. Qiu, M. S. Wilson, V. B. Eisenbeis, R. K. Harmel, E. Riemer, T. M. Haas, C. Wittwer, N. Jork, C. Gu, S. B. Shears, G. Schaaf, B. Kammerer, D. Fiedler, A. Saiardi and H. J. Jessen, *Nat. Commun.*, 2020, **11**, 6035.



32 (a) G. Ciamician and P. Silber, *Ber. Dtsch. Chem. Ges.*, 1902, **35**, 3849–4571; (b) T. Wolff and H. Görner, *Phys. Chem. Chem. Phys.*, 2004, **6**, 368–376; (c) S. Inacker, J. Fanelli, S. I. Ivlev and N. A. Hampp, *Macromolecules*, 2022, **55**, 8461–8471.

33 N. Kus, S. Breda, I. Reva, E. Tasal, C. Ogretir and R. Fausto, *Photochem. Photobiol.*, 2007, **83**, 1237–1253.

34 A. M. Schulte, G. Alachouzos, W. Szymanski and B. L. Feringa, *Chem. Sci.*, 2024, **15**, 2062–2073.

35 B. Schade, V. Hagen, R. Schmidt, R. Herbrich, E. Krause, T. Eckardt and J. Bendig, *J. Org. Chem.*, 1999, **64**, 9109–9117.

36 Q. Lin, L. Yang, Z. Wang, Y. Hua, D. Zhang, B. Bao, C. Bao, X. Gong and L. Zhu, *Angew. Chem., Int. Ed.*, 2018, **57**, 3722–3726.

37 M. Yoshimura, R. Sasayama, T. Kajiwara, C. Mori, Y. Nakasone and T. Inose, *Angew. Chem., Int. Ed.*, 2025, e202502376.

38 C. Maller, E. Marouda and M. Köhn, *ChemBioChem*, 2024, **25**, e202400561.

39 P. T. Wong, E. W. Roberts, S. Tang, J. Mukherjee, J. Cannon, A. J. Nip, K. Corbin, M. F. Krummel and S. K. Choi, *ACS Chem. Biol.*, 2017, **12**, 1001–1010.

40 C. Ji, L. Lai, P. Li, Z. Wu, W. Cheng and M. Yin, *Aggregate*, 2021, **2**, e39.

41 M. Bojtár, A. Kormos, K. Kis-Petik, M. Kellermayer and P. Kele, *Org. Lett.*, 2019, **21**, 9410–9414.

42 J. Ma, J. Wehrle, D. Frank, L. Lorenzen, C. Popp, W. Driever, R. Grosse and H. J. Jessen, *Chem. Sci.*, 2024, **15**, 6478–6487.

43 G. M. Fernandes-Cunha, C. J. McKinlay, J. R. Vargas, H. J. Jessen, R. M. Waymouth and P. A. Wender, *ACS Cent. Sci.*, 2018, **4**, 1394–1402.

44 J. P. Olson, H.-B. Kwon, K. T. Takasaki, C. Q. Chiu, M. J. Higley, B. L. Sabatini and G. C. R. Ellis-Davies, *J. Am. Chem. Soc.*, 2013, **135**, 5954–5957.

45 Q. Ding, Z. Zhang, M. Li, J.-H. Zhu, W. Fu, M. He, Y. Bai, Z. Zhang, S. Li, L. Wang, C. Deng, X. Hong, Y. Xiao and J. S. Kim, *Cell Biomater.*, 2025, **1**, 100001.

46 J. M. Baskin and C. R. Bertozzi, *QSAR Comb. Sci.*, 2007, **26**, 1211–1219.

47 A. Y. Baev, P. R. Angelova and A. Y. Abramov, *Biochem. J.*, 2020, **477**, 1515–1524.

48 T. M. Haas, S. Mundinger, D. Qiu, N. Jork, K. Ritter, T. Dürr-Mayer, A. Ripp, A. Saiardi, G. Schaaf and H. J. Jessen, *Angew. Chem., Int. Ed.*, 2022, **61**, e202112457.

49 R. H. Beddoe, D. C. Edwards, L. Goodman, H. F. Sneddon and R. M. Denton, *Chem. Commun.*, 2020, **56**, 6480–6483.

50 A. Hofer, G. S. Cremosnik, A. C. Müller, R. Giambruno, C. Trefzer, G. Superti-Furga, K. L. Bennett and H. J. Jessen, *Chem.-Eur. J.*, 2015, **21**, 10116–10122.

51 B. Amit, D. A. Ben-Efraim and A. Patchornik, *J. Chem. Soc., Perkin Trans. 1*, 1976, **1**, 57–63.

52 X. Du, H. Frei and S. H. Kim, *J. Biol. Chem.*, 2000, **275**, 8492–8500.

53 J. E. T. Corrie and G. P. Reid, *J. Labelled Compd. Radiopharm.*, 1995, **36**, 205–306.

54 G.-D. Kim, G. Liu, D. Qiu, M. G. De Leo, N. Gopaldass, J. Hermes, J. Timmer, A. Saiardi, A. Mayer and H. J. Jessen, *J. Am. Chem. Soc.*, 2025, **147**, 17626–17641.

